

Optical limiting properties of 2,6-dibromo-3,5-distyrylBODIPY dyes at 532 nm

Gugu Kubheka,^a John Mack,^{a,*} Nagao Kobayashi,^{b,*} Mitsumi Kimura^b
and Tebello Nyokong^a

^a Department of Chemistry, Rhodes University, Grahamstown 6140, South Africa

^b Department of Chemistry and Materials, Faculty of Textile Science and Technology, Shinshu University, Ueda 386-8567, Japan

This paper is dedicated to Professor Kazuchika Ohta on the occasion of his retirement.

Received 4 May 2017

Accepted 30 June 2017

ABSTRACT: Optical limiting properties of 2,6-dibromo-3,5-distyrylBODIPY dyes were investigated by using the z-scan technique at 532 nm in the nanosecond pulse range. A strong reverse saturable absorption response was observed even in solution, which suggests that compounds of this type are potentially suitable for use in optical limiting applications.

KEYWORDS: BODIPYs, Knoevenagel condensation, nonlinear optics, optical limiting, z-scan.

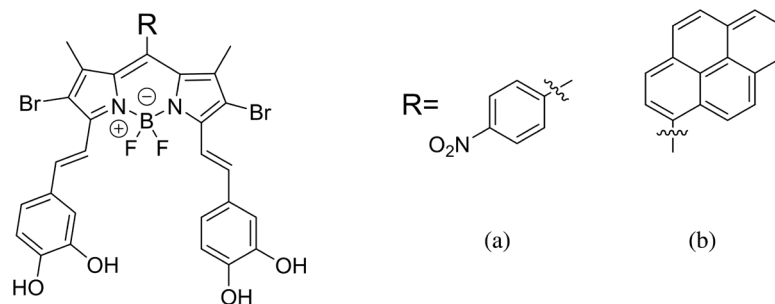
INTRODUCTION

Optical limiting (OL) materials are useful in applications, since they can protect the human eye and sensitive optical devices from intense incident laser beams [1–3]. OL can depend on nonlinear absorption, scattering, or refraction with nonlinear absorption (NLA) usually being the main focus when molecular dyes are involved as is the case in this study. The second harmonic of Nd/YAG laser systems at 532 nm is particularly important in this regard [4–7]. Ideally, there should be high transmittance of low-intensity light, along with the attenuation of the incident laser beam, in a manner that limits the output fluence [1–3]. In recent years, there has been a strong focus on the OL properties of phthalocyanines [8–10], porphyrins [8, 11], fullerenes [1], carbon nanotubes [12], nanoparticles [13], metal nanowires [14] and other organic chromophores [15, 16]. The most important mechanisms that are involved in achieving optical limiting are NLA, nonlinear refraction and nonlinear light scattering [17, 18]. Solutions of molecular dyes such as porphyrins and phthalocyanines

with a positive NLA coefficient exhibit reverse saturable absorption (RSA) with a decrease in transmittance at high-intensity levels [16], and hence function as optical limiters at wavelengths where there is only very limited absorbance under ambient light conditions. Two-photon absorption (2PA) is a resonant third-order nonlinear optical (NLO) process in which an excited state is formed by the simultaneous absorption of two photons of half-energy, in an intense focused light beam such as that generated by a laser source, and is described by the imaginary part of the third-order susceptibility $\text{Im}[\chi^{(3)}]$ and second-order hyperpolarizabilities (γ) [19, 20]. The main goal in research on optical limiters is to identify materials that can maximize these two NLO parameters. The focus in this study is an investigation of the optical limiting that results from NLA processes at 532 nm when boron dipyrromethene (BODIPY) dyes with extended π -conjugation systems are used in this context.

BODIPY dyes have been considered for a wide range of applications, due to their facile synthesis and structural modification, high molecular extinction coefficients and photostability [21]. They would not normally be considered for use as optical limiters in the context of the second harmonic of Nd/YAG lasers, however, since they typically absorb strongly in the green portion of

* Correspondence to: Dr. John Mack, email: j.mack@ru.ac.za; Prof. Nagao Kobayashi, email: nagaok@shinshu_u.ac.jp.



Scheme 1. The structures of the 2,6-dibromo-3,5-distyrylBODIPY dyes that were synthesized in this work for NLO studies

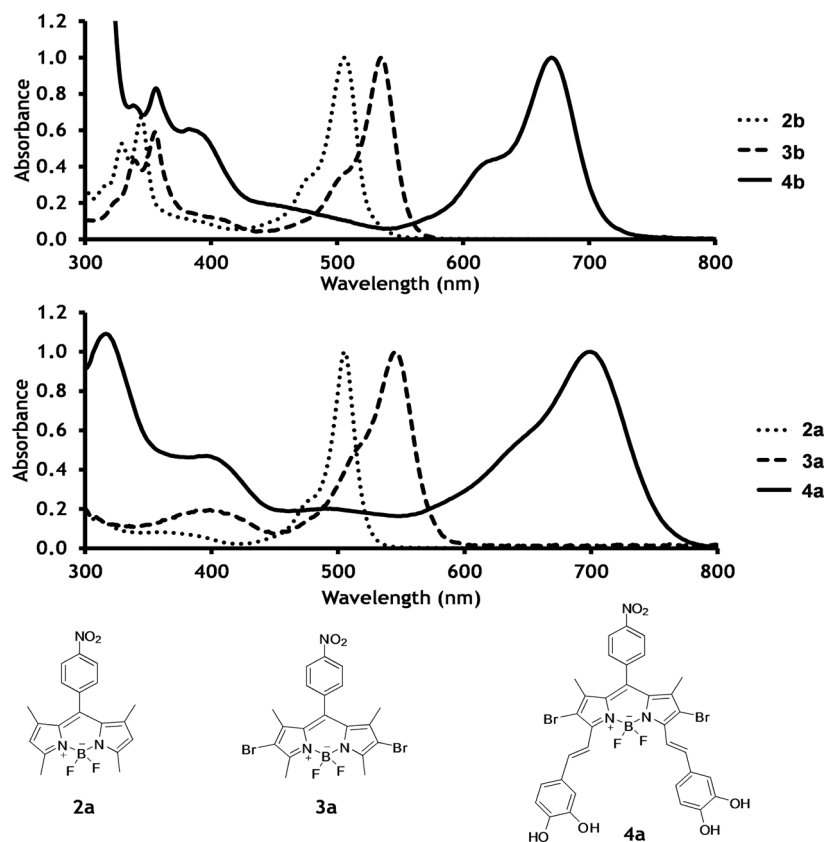
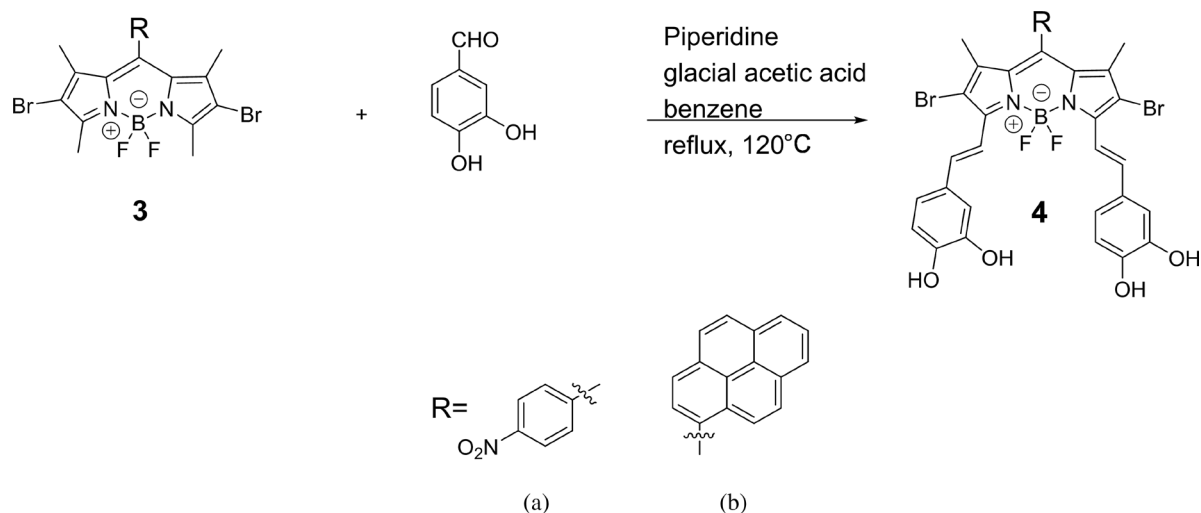


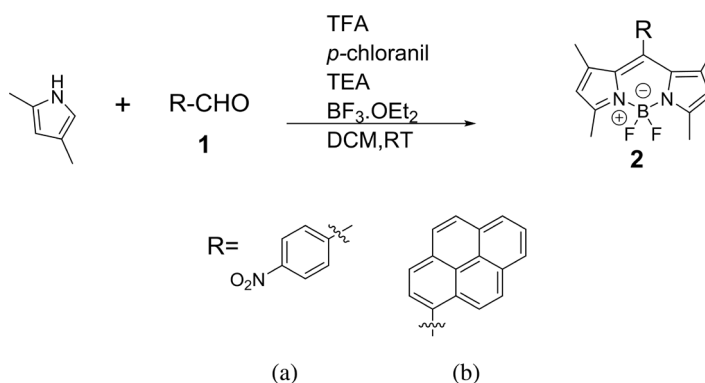
Fig. 1. Normalized absorption spectra of **2a–4a** (BOTTOM) and **2b–4b** (TOP) in CH_2Cl_2 . Details for the main spectral bands are provided in Table 1

the visible region. Structural analogs of BODIPY dyes, such as 3,5-distyryl-BODIPYs (Scheme 1) have optical properties that are substantially modified and hence more suitable for OL applications at 532 nm, however. The extension of the π -conjugation system shifts the main BODIPY spectral bands to longer wavelength, and this leads to relatively weak absorption at 532 nm (Fig. 1), making the dyes potentially suitable for OL where the second harmonic of Nd/YAG lasers is concerned. It has previously been demonstrated that π -conjugation systems possess large electronic polarizabilities, and hence it is reasonable to expect conjugated molecules to possess the substantial second-order hyperpolarizabilities that enhance the OL properties [22, 23]. Molecules with

donor and acceptor moieties that are separated by a π -conjugation system (D- π -A) are also known to exhibit large third order susceptibility values [19]. In this study, 3,5-distyryl-BODIPY dyes with *meso*-pyrene and *meso*-4-nitrophenyl rings have been studied to assess their potential for OL applications. Two novel distyryl-BODIPY dyes were synthesized (Scheme 2) with electron withdrawing bromine atoms at the 2,6-positions and π -conjugation systems extended with electron donating dihydroxystyryl moieties at the 3,5-positions. There have been relatively few previous studies on the use of BODIPY dyes and their analogs as OL materials for 532 nm excitation pulses [24–26] and those at other wavelengths [27–29].



Scheme 2. The synthesis of **4a** and **4b** via Knoevenagel condensation reactions



Scheme 3. The synthetic procedure for **2a** and **2b**

EXPERIMENTAL

Materials

2,4-Dimethylpyrrole, 4-nitrobenzaldehyde reagent plus (98%), 1-pyrenecarboxaldehyde reagent plus (99%), trifluoroacetic acid (TFA), *p*-chloranil, triethylamine (TEA), boron trifluoride diethyl etherate ($\text{BF}_3 \cdot \text{OEt}_2$), bromine, sodium thiosulfate, glacial acetic acid and piperidine were purchased from Sigma-Aldrich. Hydrochloric acid (32%) was purchased from Merck. All solvents were dried using molecular sieves before use.

Instrumentation

UV-visible absorption spectra were recorded on a Shimadzu UV-2550 spectrophotometer. Fluorescence emission spectra were measured on a Varian Eclipse spectrofluorimeter. The *z*-scan experiments were performed using a frequency-doubled Quanta-Ray Nd:YAG laser as the excitation source. The laser was operated in a near Gaussian transverse mode at 532 nm (second

harmonic), with a pulse repetition rate of 10 Hz and an energy range of 0.1 μJ –0.1 mJ limited by the energy detectors (Coherent J5–09). The low repetition rate of the laser prevents the build up of thermal nonlinearities. The beam was filtered spatially to remove higher order modes and tightly focused with a 15 cm focal length lens. A 2 mm quartz cuvette was used to measure *z*-scan data in solution.

Synthesis

2a and **2b** were synthesized by modified versions of methods that have been described previously (Scheme 3) [30, 31]. 2,4-Dimethylpyrrole (2 g, 21.02 mmol) and the appropriate benzaldehyde (10.51 mmol) were dissolved in dry CH_2Cl_2 (117.4 ml) under argon. TFA (0.2 ml) was added, and the reaction mixture was stirred at room temperature. When the aldehyde was consumed (monitored by TLC), a solution of *p*-chloranil (3.88 g, 15.77 mmol) in dry CH_2Cl_2 (5 ml) was added *via* syringe at 0°C. After stirring for 20 min at room temperature, TEA (10.64 g, 105.10 mmol) and $\text{BF}_3 \cdot \text{OEt}_2$ (17.90 g, 126.12 mmol) were added

dropwise at 0°C over a period of 10 min, and the mixture was stirred at room temperature for 18 h. The mixture was then filtered and washed with water (6 × 60 ml), dried over anhydrous sodium sulfate and the solvent was removed by using a rotary evaporator. The residue was purified by flash column chromatography by eluting with 1:4 CH₂Cl₂:ethyl acetate to yield the pure products as orange crystalline solids.

2a: Yield 0.65 g (41%). Anal. calc. for C₁₉H₁₈BF₂N₃O₂: C, 61.82; H, 4.91; N, 11.38%. Found: C, 61.80.96; H, 4.50; N, 10.98. ¹H NMR (600 MHz; CDCl₃): δ, ppm 1.33 (6H, s, 2 × CH₃), 2.53 (6H, s, 2 × CH₃), 6.01 (2H, s, 2 × CH), 7.51 (2H, d, J = 12 Hz, 2 × Ar–H), 8.34 (2H, d, J = 12 Hz, 2 × Ar–H). IR: ν, cm⁻¹ 3106 (Ar C–H), 2920–2851 (Aliph C–H), 1604 (Ar C–C), 1525 (Ar N–O). MS (ESI): m/z 369.15 (calcd. [M]⁺ 369.12).

2b: Yield 0.63 g (63%). Anal. Calc. for C₂₉H₂₃BF₂N₂: C, 77.69; H, 5.17; N, 6.25%. Found: C, 77.62; H, 5.13; N, 6.20. ¹H NMR (600 MHz; CDCl₃): δ, ppm 1.20 (3H, s, CH₃), 1.42 (3H, s, CH₃), 2.55 (3H, s, CH₃), 2.75 (3H, s, CH₃), 5.95 (2H, s, 2 × CH), 7.76 (H, s, Ar–CH), 7.84 (H, s, Ar–CH), 7.98 (H, s, Ar–H), 8.12 (2H, d, J = 18 Hz, 2 × Ar–H), 8.35 (2H, d, J = 24 Hz, 2 × Ar–H), 8.47 (2H, d, J = 18 Hz, 2 × Ar–H). IR: ν, cm⁻¹ 3179 (Ar C–H), 2920–2850 (Aliph C–H), 1600 (Ar C–C). MS (ESI): m/z 448.32 (calcd. [M]⁺ 448.35).

3a and **3b** were prepared by following modified versions of a procedure reported previously (Scheme 4) [32]. To a solution of BODIPY **2a** or **2b** (0.33 mmol) in 62 mL of dry CH₂Cl₂, liquid bromine (24 μl, 0.48 mmol) in CH₂Cl₂ (6 mL) was added at 0°C over a period of 2 h, and the mixture was left to stir at room temperature overnight. The mixture was washed with an aqueous solution of sodium thiosulfate and extracted with CH₂Cl₂. The organic layers were combined, dried over Na₂SO₄, and evaporated to dryness. Purification was performed by column chromatography on silica gel by using CH₂Cl₂:hexane (8:1) as the eluent. The target compounds were obtained as red solids.

3a: Yield 0.091 g (78%). Anal. calc. for C₁₉H₁₆BBR₂F₂N₃O₂: C, 43.31; H, 3.06; N, 7.97%. Found: C, 48.01; H, 4.10; N, 7.79. ¹H NMR (400 MHz; CDCl₃): δ, ppm 1.26 (6H, s, 2 × CH₃), 1.36 (3H, s, CH₃), 1.39 (3H, s, CH₃), 7.55 (2H, d, J = 8.0 Hz, 2 × Ar–H), 8.45 (2H, d, J = 8.0 Hz, 2 × Ar–H). IR: ν, cm⁻¹ 3111 (Ar C–H), 2922–2852 (Aliph C–H), 1599 (Ar C–C), 1521 (Ar N–O). MS

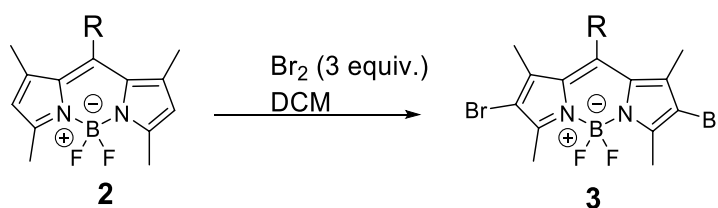
(MALDI-TOF): m/z 524.97 (calcd. for [M]⁺ 524.33).

3b: Yield 0.098 g (89%). Anal. calc for C₂₉H₂₁BBR₂F₂N₂: C, 57.47; H, 3.49; N, 4.62%. Found: C, 57.50; H, 3.43; N, 4.55. ¹H NMR (CDCl₃): δ, ppm 1.22 (3H, s, CH₃), 1.52 (3H, s, CH₃), 2.65 (3H, s, CH₃), 2.95 (3H, s, CH₃), 7.88 (H, s, CH), 7.95 (H, s, CH), 7.99 (H, s, CH), 8.24 (2H, d, J = 18 Hz, 2 × Ar–H), 8.42 (2H, d, J = 24 Hz, 2 × Ar–H), 8.56 (2H, d, J = 18 Hz, 2 × Ar–H). IR: ν, cm⁻¹ 3293 (Ar C–H), 2921–2851 (Aliph C–H), 1600 (Ar C–C). MS (MALDI-TOF): m/z 604.01 (calcd. for [M–F]⁺ 589.20).

4a and **4b** were synthesized following a modified version of the Knoevenagel condensation method [33, 34]. A mixture of BODIPY **3a** or **3b** (120 mg, 0.14 mmol), 3,4-dihydroxybenzaldehyde (59 mg, 0.2 mmol), glacial acetic acid (0.4 mL), piperidine (0.4 mL), was refluxed in benzene (50 mL) until the aldehyde was consumed. The water formed during the reaction was removed azeotropically with a Dean–Stark trap apparatus. The mixture was concentrated under reduced pressure. The residue was then purified by silica gel column chromatography by using CH₂Cl₂:MeOH (97:3) as the eluent. Green colored fractions were collected, and the solvent was removed with a rotary evaporator to afford the desired products as green solids.

4a: Yield 0.042 g (35%). Anal. calc. for C₃₃H₂₄BBR₂F₂N₃O₆: C, 51.66; H, 3.15; N, 5.48%. Found: C, 51.76; H, 4.02; N, 5.60. ¹H NMR (600 MHz, DMSO-*d*₆): δ, ppm 1.96 (6H, s, 2 × CH₃), 6.91 (4H, d, J = 6.0 Hz, 4 × Ar–H), 7.24 (6H, m, 6 × Ar–H); 7.27 (2H, d, J = 6.0 Hz, 2 × Ar–H), 7.29 (2H, d, J = 6.0 Hz, 2 × Ar–H), 9.70 (4H, s, 4 × Ar–OH). IR: ν, cm⁻¹ 3322 (O–H), 2955 (Ar C–H), 2916–2849 (Aliph C–H), 1463 (Ar C–C), 1306 (Ar N–O). UV-Vis (EtOH): λ_{max}, nm (log ε) 700 (4.98), 635 (4.74), 508 (4.35), 407 (4.68), 323 (4.02). MS (MALDI-TOF): m/z 767.18 (calcd. for [M]⁺ 767.69).

4b: Yield 0.055 g (55%). Anal. calc. for C₄₃H₂₉BBR₂F₂N₂O₄: C, 61.03; H, 3.45; N, 3.31%. Found: C, 61.23; H, 4.01; N, 3.35. ¹H NMR (600 MHz, DMSO-*d*₆): δ, ppm 2.65 (6H, s, 2 × CH₃), 6.98 (4H, d, J = 6.0 Hz, 4 × Ar–H), 7.30 (6H, m, 6 × Ar–H), 8.27 (3H, m, 3 × Ar–H), 8.45 (4H, m, 4 × Ar–H), 8.66 (2H, d, J = 18 Hz, 2 × Ar–H), 9.84 (4H, s, 4 × Ar–OH). IR: ν, cm⁻¹ 3204 (O–H), 3053 (Ar C–H), 2920–2875 (Aliph C–H), 1591 (Ar C–C). UV-Vis (EtOH): λ_{max}, nm (log ε) 690 (4.89), 620 (4.42), 503 (4.24), 419 (4.48), 356 (4.81), 320 (4.12). MS (MALDI-TOF): m/z; 846.33 (calcd. for [M]⁺ 847.10).



Scheme 4. The synthetic procedure for **3a** and **3b**. The –R groups at the *meso*-positions are the same as those shown in Schemes 1–3.

RESULTS AND DISCUSSION

Synthesis and characterization

BODIPYs are conventionally prepared through an acid-catalyzed condensation reaction of a pyrrole ring with an aromatic aldehyde (**1**) [35]. 2,4-Dimethylpyrrole is usually preferred as a starting material, since the methyl-substituents prevent the formation of porphyrins. The 1,3,5,7-tetramethylBODIPYs (**2**) that are formed in this manner can be readily brominated at the 2,6-positions with liquid bromine. The introduction of styryl groups was achieved by reacting an aromatic aldehyde with the appropriate 2,6-dibromoBODIPY (**3**) to form (Scheme 2) through Knoevenagel condensation reactions [33, 34]. Styrylation is one of the most useful strategies for shifting the main spectral band of the BODIPY chromophore to the red (Fig. 1) [36]. The protons attached to the methyl groups are acidic enough to undergo condensation reactions and form the target BODIPY dyes (**4**). Extension of the π -conjugation and the addition of functionality is most frequently accomplished through the methyl groups at the 3,5-positions, since this generally produces a greater red shift (*ca.* 50–100 nm) than is observed upon extending the π -conjugation through the 2,6- or 1,7-positions [37]. The smaller red shift observed upon bromination (Fig. 1) can be attributed to a narrowing of the HOMO–LUMO gap due to the effect of the lone pairs on the bromine atoms [38], since the HOMO has large molecular orbital coefficients at the 2,6-positions of the BODIPY core. The formation of the target compounds was confirmed by the absence of the 2,6-position proton signals in the ^1H NMR spectrum (Fig. 2) and the presence of bands related to the hydroxyl groups in the ^1H NMR and IR spectra (Figs 2 and 3).

Very low fluorescence (Φ_{F}) and singlet oxygen quantum (Φ_{Δ}) yields (Table 1) were obtained for **4a** and **4b** by using comparative methods [39, 40] by making use of zinc phthalocyanine as the standard with diphenylisobenzofuran used as the $^1\text{O}_2$ scavenger in the latter case. The solvent dependence of the fluorescence quantum yield values was not studied in depth due to the unusually low values that were obtained, which may be related to intramolecular charge transfer character that is introduced into the S_1 excited state by the electron donating hydroxyl substituents on the styryl moieties, since this enhances the rate of non-radiative decay [34, 36, 37]. The addition of bromine atoms at the 2,6-positions would normally be expected to introduce a large heavy atom effect that would result in large singlet oxygen quantum yield values even in the context of 2,6-distyryl dyes [41], but this was not observed for **4a** and **4b** (Table 1). No evidence of aggregation was observed when Beer–Lambert analyses were carried out to determine the extinction coefficients of **4a** and **4b**.

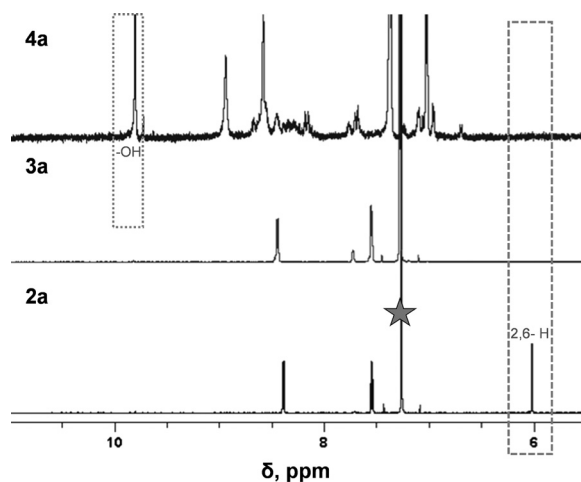


Fig. 2. The aromatic region of the ^1H NMR spectra of **2a**, **3a** and **4a** in CDCl_3 and $\text{DMSO}-d_6$. The dashed box highlights the disappearance of the 2,6-position proton signal in the spectra of **3a** and **4a**, while a dotted box is used for the OH proton signals of **4a**. A gray star is used to highlight the solvent signal of CDCl_3 .

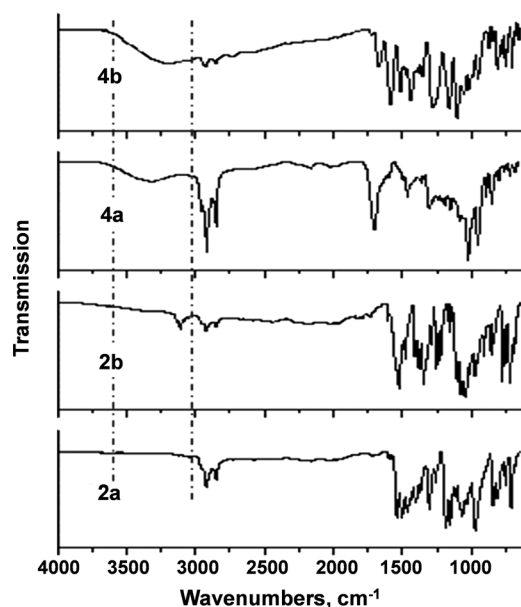


Fig. 3. The IR spectra of **2a**, **2b**, **4a** and **4b**. The broad OH stretch bands of **4a** and **4b** are highlighted with dashed lines.

Table 1. Photophysical properties of **4a** and **4b** in CH_2Cl_2

Sample	Solvent	λ_{abs} (nm)	λ_{ex} (nm)	$\log \epsilon$	Φ_{F}	Φ_{Δ}
4a	CH_2Cl_2	700	738	4.98	0.004	n.d. ^a
4b	CH_2Cl_2	670	699	4.89	0.020	n.d. ^a

^an.d. implies that the value is too low to be detectable.

NLO parameters

Open aperture z-scan measurements were performed according to the method described by Sheik-Bahae and co-workers [20, 42, 43] (Eqs. 1–3):

$$T(z) = \frac{1}{\sqrt{\pi}q_0(z)} \int_{-\infty}^{\infty} \ln[1 + q_0(z)e^{-\tau^2}] d\tau \quad (1)$$

where

$$q_0(z) = \frac{\beta_{\text{eff}} I_{00} L_{\text{eff}}}{1 + \frac{z^2}{z_0^2}} \quad (2)$$

and

$$L_{\text{eff}} = \frac{1 - e^{-\alpha L}}{\alpha} \quad (3)$$

and $T(z)$, L and I_{00} are the transmission, pathlength and on-focus peak input irradiance, respectively; α and β_{eff} are the linear and effective nonlinear absorption coefficients; and L_{eff} , z , and z_0 are the effective pathlength, the translation distance of the sample relative to the focal point of the z-scan measurements, and the Rayleigh length, respectively. The Rayleigh length is defined as $(\pi w_0^2)/\lambda$, where λ is the wavelength of the laser beam and w_0 is the beam waist at the focus ($z = 0$), which is defined as the distance from the beam center to the point where the intensity reduces to $1/e^2$ of its on axis value.

Equation 4 provides a numerical form of Eq. 1, and is employed as a fit function to the experimental data [20, 42, 43].

$$T(z) = 0.363e^{\left(\frac{-q_n(z)}{5.60}\right)} + 0.286e^{\left(\frac{-q_n(z)}{1.21}\right)} + 0.213e^{\left(\frac{-q_n(z)}{24.62}\right)} + 0.096e^{\left(\frac{-q_n(z)}{115.95}\right)} + 0.038e^{\left(\frac{-q_n(z)}{965.08}\right)} \quad (4)$$

The imaginary component of the third-order susceptibility ($\text{Im}[\chi^{(3)}]$) depends on the speed of the NLA response and is related to the β_{eff} value through Eq. 5 [44]:

$$\text{Im}[\chi^{(3)}] = \frac{n^2 \epsilon_0 c \lambda \beta_{\text{eff}}}{2\pi} \quad (5)$$

where n , c and ϵ_0 are the linear refractive index, the speed of light, and the permittivity of free space, respectively.

The second-order hyperpolarizability (γ) values of the materials, which describe the interaction of the incident photons with the permanent dipole moment of the dyes, were calculated using Eq. 6 [9, 45].

$$\gamma = \frac{\text{Im}[\chi^{(3)}]}{f^4 C_{\text{mol}} N_A} \quad (6)$$

where N_A is the Avogadro constant, C_{mol} is the molar concentration of the active chromophore, and f is the Lorentz local field factor, which is defined as $f = (n^2 + 2)/3$.

The open aperture z-scan method was used to characterize the OL properties of the 3,5-distyryl-BODIPY dyes selected for this study on the nanosecond timescale. The nonlinear absorption coefficient (β) is an important parameter for assessing the suitability of materials for OL applications, since it provides a wavelength-dependent measure of the degree of nonlinear absorptivity for the material being studied. Generally, this parameter depends on 2PA [18, 44], but when nanosecond pulses are used, as is the case in this study, excited state absorption (ESA) can also occur in addition to 2PA, so an effective nonlinear absorption coefficient (β_{eff}) is derived rather than the intrinsic β value that is associated with 2PA alone. When absorption of the incident 532 nm light by an excited state is more prominent than that of the ground state, ESA from excited states that are populated via 2PA can lead to the strong RSA response that is required for optical limiting. The 2PA and ESA mechanisms result in a decrease in transmittance as the material approaches the zero position of the z-scan measurements due to the RSA response, since there are higher incident light levels at the focal point of the lens that is used [46].

Z-scan measurements for **4a** and **4b** were carried out in CH_2Cl_2 , Table 2. Figure 4 shows representative open-aperture z-scans that were obtained at 532 nm by using 10 ns laser pulses. The measurements demonstrate that there is strong NLA behavior, with the shapes of the z-scan profile exhibiting RSA signatures. Analyses of the z-scan results to obtain β_{eff} values were carried out by fitting the data to the 2PA-assisted ESA function described in Eqs. 1–4. The β_{eff} values (Table 2) lie within the range

Table 2. Optical limiting properties of **4a** and **4b** in CH_2Cl_2 solution obtained with 10 ns pulses at 532 nm

Sample	Solvent	Conc. (M) ^a	β_{eff} (cm.GW ⁻¹)	I_{lim} (J.cm ⁻²)	$\text{Im}[\chi^{(3)}]$ (esu)	γ (esu)	I_{00} (MW.cm ⁻²)
4a	CH_2Cl_2	0.0727	300	0.73	6.53×10^{-10}	4.59×10^{-30}	3.42
4b	CH_2Cl_2	0.263	179	1.02	3.89×10^{-10}	7.57×10^{-31}	3.00

^aDiffering concentrations were used so the absorbance values of the **4a** and **4b** solutions were similar at 532 nm.

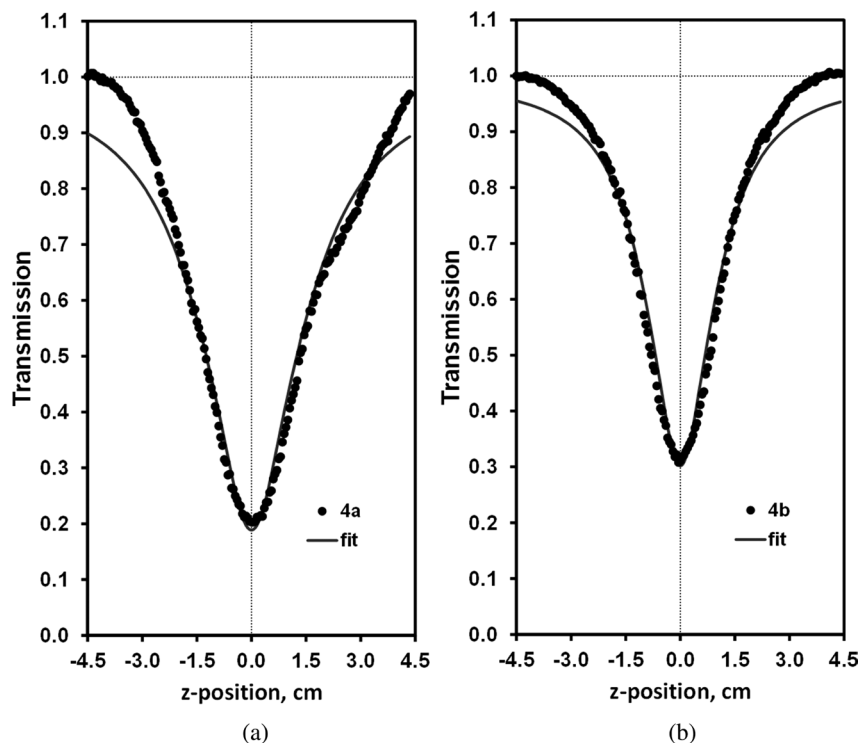


Fig. 4. Open-aperture z-scans for (a) **4a** and (b) **4b** measured in CH_2Cl_2 . Detailed NLO parameters are provided in Table 2

previously reported values for other organic compounds [44], so **4a** and **4b** can be viewed as being promising OL materials as they are able to reduce the transmission of the incident laser light to well below 50% (Fig. 4). It is noteworthy that this happens in solution, since organic dyes often have to be conjugated to nanomaterials or embedded in polymer thin films for this to be achieved [16] and to achieve a sufficiently large RSA response to form an effective OL material. The unusually strong RSA responses for **4a** and **4b** can be attributed to the increased polarizability due to the enhanced dipole moments when the BODIPY dye has a D- π -A substitution pattern (Scheme 1). The results obtained for **4a** lie significantly below this limiting threshold. The 4-nitrophenyl *meso*-substituent of **4a** is more strongly withdrawing than the pyrenyl substituent of **4b**, so greater D- π -A character is anticipated that would be expected to result in a stronger RSA response.

The limiting threshold fluence (I_{lim}) is an important parameter in OL measurements. It is defined as the input fluence at which the nonlinear transmittance is 50% of the linear transmittance. The value of I_{lim} can be determined by using the plot of transmission vs. input fluence (Fig. 5). The limiting threshold for damage to the human eye is $0.95 \text{ J}\cdot\text{cm}^{-2}$ [47]. Thus, I_{lim} values of below $0.95 \text{ J}\cdot\text{cm}^{-2}$ are an indication of a good NLO response to the input intensity. None of the RSA responses of BODIPY dyes that have been reported previously at 532 nm have resulted in nonlinear transmittance values of below 50%

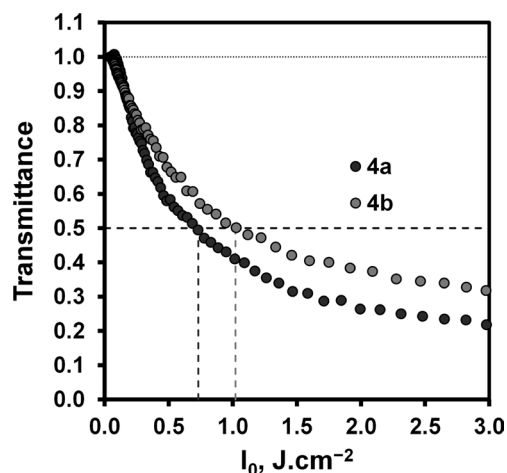


Fig. 5. Transmittance vs. input fluence (I_0) curves for **4a** and **4b** calculated from the z-scan measurements in CH_2Cl_2 . Detailed NLO parameters are provided in Table 2. The calculations for the I_{lim} values are shown with vertical lines

during z-scan measurements [25, 26]. Saturation fluence curves for the BODIPY dyes are compared by plotting transmittance against the input fluence (I_0) (Fig. 6) demonstrate that the optical limiting effect is maintained at higher I_0 values.

The estimated γ and $\text{Im}[\chi^{(3)}]$ values for the samples are provided in Table 2. The γ values provide a measure of the interaction of the incident photon with the

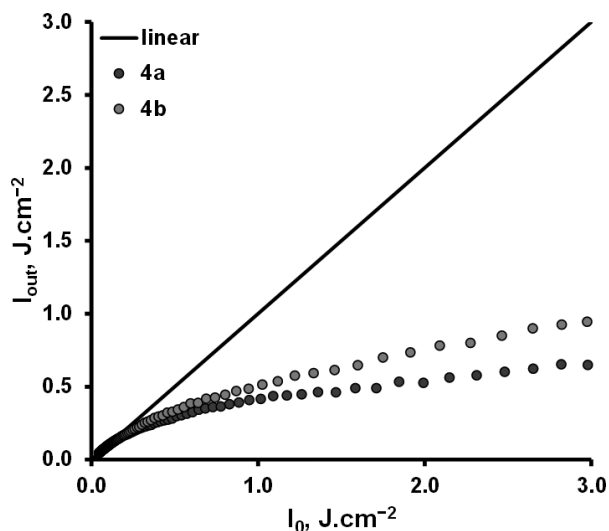


Fig. 6. Output fluence (I_{out}) vs. input fluence (I_0) curves for **4a** and **4b** calculated from the z-scan measurements in CH_2Cl_2 . Detailed NLO parameters are provided in Table 2

permanent dipole moments of **4a** and **4b**. The larger value obtained for **4a** is preferred and is related to the electron withdrawing NO_2 group on the *meso*-aryl substituent, since this should result in a stronger permanent dipole moment. The $\text{Im}[\chi^{(3)}]$ values, which are an intrinsic property of OL materials at the wavelength of incident laser light that is being studied, are related to the rate of non-linear response to the intense incident laser pulses with **4a** again having the larger value. The $\text{Im}[\chi^{(3)}]$ and γ values of **4a** (Table 2) fall well within the reported ranges that have been reported previously for OL materials of 10^{-9} to 10^{-15} esu for $\text{Im}[\chi^{(3)}]$ and of 10^{-29} to 10^{-34} esu for γ [48]. This demonstrates that 2,6-dibromo-3,5-distyryl-BODIPY derivatives with D- π -A substitution properties have promising OL properties and merit further in-depth investigation.

CONCLUSIONS

Open aperture z-scan studies on the nanoscale timescale demonstrate that 2,6-dibromo-3,5-distyryl-BODIPY dyes have relatively strong OL properties at an excitation wavelength of 532 nm making them potentially suitable for optical limiting applications. This study provides the first example of nonlinear transmittance of below 50% being achieved at 532 nm with a BODIPY dye. The I_{lim} value of **4a** in CH_2Cl_2 is significantly below the threshold value that has been reported for damage to the human eye of 0.95 J.cm^{-2} and comparable work on phthalocyanines and their analogs [49–51] suggests that further improvements could be achieved in this regard if the dye were to be embedded into polymer thin films as would be the case in practical applications for protecting the vision of pilots and sensitive optical devices. The key structural difference between the dyes was that **4a** has an electron withdrawing *meso*-nitrophenyl group,

while **4b** has a *meso*-pyrenyl group. The differences observed in the OL parameters demonstrate that relatively minor structural changes such as this can have a significant effect on the NLO properties of BODIPY dyes with D- π -A structures. Further studies are already in progress to determine how the structure of the BODIPY chromophore can be further modified to further improve the OL properties at 532 nm.

Acknowledgements

This work was partially supported by a bilateral program between the Japan Society for the Promotion of Science (JSPS) and National Research Foundation (NRF) of South Africa (uid: 92425), JSPS KAKENHI grant numbers JP15H02172 & JP15H0091, an NRF of South Africa CSUR grant (uid: 93627) and a DAAD-NRF in-country doctoral scholarship to GK. Photophysical measurements were made possible by the Laser Rental Pool Programme of the Council for Scientific and Industrial Research (CSIR) of South Africa.

References

1. Tutt LW, Kost A. *Nature* 1992; **356**: 225–226.
2. Perry JW, Mansour K, Lee IYS, Wu XL, Bedworth PV, Chen CT, Ng D, Marder SR, Miles P, Wada T, Tian M and Sasabe H. *Science* 1996; **273**: 1533–1536.
3. Lim GK, Chen ZL, Clark J, Goh RGS, Ng WH, Tan HW, Friend RH, Ho PKH and Chua LL. *Nature Photonics* 2011; **5**: 554–560.
4. Shirk J, Pong RGS, Bartoli FJ and Snow AW. *Appl. Phys. Lett.* 1993; **63**: 1880–1882.
5. Perry JW, Mansour K, Marder SR, Perry KJ, Alvarez D Jr and Choong I. *Opt. Lett.* 1994; **19**: 625–627.
6. Hughes S, Spruce G, Wherrett BS and Kobayashi T. *J. Appl. Phys.* 1997; **81**: 5905–5912.
7. Shirk JS, Pong RGS, Flom SR, Heckmann H and Hanack M. *J. Phys. Chem. A* 2000; **104**: 1438–1449.
8. Calvete M, Yang GY and Hanack M. *Synth. Met.* 2004; **141**: 231–243.
9. Chen Y, Hanack M and Araki Y, Ito O. *Chem. Soc. Rev.* 2005; **34**: 517–529.
10. Chen Y, Hanack M, Blau WJ, Dini D, Liu Y, Lin Y and Bai J. *J. Mater. Sci.* 2006; **41**: 2169–2185.
11. Senge MO, Fazekas M, Notaras EGA, Blau WJ, Zawadzka M, Locos OB and NiMhuircheartaigh EM. *Adv. Mater.* 2007; **19**: 2737–2774.
12. Chen P, Wu X, Sun X, Lin J, Ji W and Tan KL. *Phys. Rev. Lett.* 1999; **82**: 2548–2551.
13. Sun YP, Riggs JE, Rollins HW and Guduru R. *J. Phys. Chem. B* 1999; **103**: 77–82.
14. Han YP, Luo MH, Wang QW, Wang JX and Gao XL. *Adv. Mater. Res.* 2011; **295**: 152–155.
15. Zheng QD, Gupta SK, He GS, Tan LS and Prasad PN. *Adv. Funct. Mater.* 2008; **18**: 2770–2779.

16. Dino D, Calvete MFJ and Hanack M. *Chem. Rev.* 2016; **116**: 13043–14276.
17. Tutt LW and Boggess TF. *Progress in Quantum Electronics* 1993; **17**: 299–338.
18. Wang J and Blau WJ. *J. Opt. A* 2009; **11**: 024001.
19. Sutherland RL. In *Handbook of Nonlinear Optics*, 2nd ed.; Marcel Dekker: New York, NY, 2003.
20. Van Stryland EW and Sheik-Bahae M. In *Characterization Techniques and Tabulations for Organic Nonlinear Materials*; Kuzyk MG and Dirk CW (Eds.); Marcel Dekker, Inc.: New York, 1998; pp. 655–692.
21. Kubo Y, Watanabe K, Nishiyabu R, Hata R, Murakami A, Shoda T and Ota H. *Org. Lett.* 2011; **13**: 4574–4577.
22. Ortiz A, Insuasty B, Torres MR, Herranz MR, Herranz NMA and Martin N and Viruela R. *Eur. J. Org. Chem.* 2008; 99–108.
23. Marder SR and Beratan DN and Cheng LT. *Science* 1991; **252**: 103–106.
24. Frenette M, Hatamimoslehabadi M, Bellinger-Buckley S, Laoui S, La J, Bag S, Mallidi S, Hasan T, Bouma B, Yelleswarapu C and Rochford J. *J. Am. Chem. Soc.* 2014; **136**: 15853–15856.
25. Kulyk B, Taboukhat S, Akdas-Kilig H, Fillaut J-L, Boughaleb Y and Sahraoui B. *RSC Adv.* 2016; **6**: 84854–84859.
26. Zhu M, Yuan M, Liu X, Ouyang C, Zheng H, Yin X, Zuo Z, Liu H and Li Y. *J. Polym. Sci. A* 2008; **46**: 7401–7410.
27. Kulyk B, Taboukhat S, Akdas-Kilig H, Fillaut J-L, Karpierz M and Sahraoui B. *Dyes Pigm.* 2017; **137**: 507–511.
28. Zheng Q, He GS and Prasad PN. *Chem. Phys. Lett.* 2009; **475**: 250–255.
29. Bouit P, Kamada K, Feneyrou P, Berginc G, Toupet L, Maury O and Andraud C. *Adv. Mater.* 2009; **21**: 1151–1154.
30. de Rezende LCD, Vaidergorn MM, Moraes JCB and da Silva Emery F. *J. Fluoresc.* 2014; **24**: 257–266.
31. Yang Y, Zhang L, Gao C, Xu L, Bai SX and Liu X. *RSC Adv.* 2014; **4**: 38119–38123.
32. Jiao L, Pang W, Zhou J, Wei Y, Mu X, Bai G and Hao E. *J. Org. Chem.* 2011; **76**: 9988–9996.
33. Rurack K, M. Kollmannsberger M and Daub J. *Angew. Chem., Int. Ed.* 2001; **40**: 385–387.
34. Wang S, Liu H, Mack J, Tian J, Zou B, Lu H, Li Z, Jiang J and Shen Z. *Chem. Commun.* 2015; **51**: 13389–13392.
35. Loudet A and Burgess K. *Chem Rev.* 2007; **107**: 4891–4932.
36. Lu H, Mack J, Yang Y and Shen Z. *Chem. Soc. Rev.* 2014; **43**: 4778–4823.
37. Gai L, J. Mack J, Lu H, Yamada H, Lai G, Li Z and Shen Z. *Chem. Eur. J.* 2014; **20**: 1091–1102.
38. Kubheka G, Uddin I, Amahuya E, Mack J and Nyokong T. *J. Porphyrins Phthalocyanines* 2016; **20**: 1016–1024.
39. Frey-Forgues S and Lavabre D. *J. Chem. Ed.* 1999; **76**: 1260–1264.
40. Seotsanyana-Mokhosi I and Nyokong T. *J. Porphyrins Phthalocyanines* 2004; **8**: 1214–1221.
41. Ngoy BP, Molupe N, Harris J, Fomo G, Mack J and Nyokong T. *J. Porphyrins Phthalocyanines* 2017; **21**: 431–438.
42. Sheik-Bahae M, Said AA, Wei T-H, Hagan DJ and Van Stryland EW. *IEEE, J. Quantum Electron.* 1990; **26**: 760–769.
43. Sheik-Bahae M, Said AA and Van Stryland EW. *Opt. Lett.* 1989; **14**: 955–957.
44. D. Dini and M. Hanack. In *The Porphyrin Handbook*; K. M. Kadish, K. M. Smith and R. Guillard (Eds.); Academic Press: USA. 2003; Vol. 17, pp. 22–31.
45. de la Torre G, Vázquez P, Agulló-López F and Torres T. *Chem. Rev.* 2004; **104**: 3723–3750.
46. Saleh BEA and Teich MC. *Fundamentals of Photonics*, Wiley, New York, 1991.
47. Matthes R. *Int. Comm. Health Phys.* 2000; **79**: 431–440.
48. Pritchett T, in *Sensors and Electron Devices Directorate*, Army Research Laboratory, Adelphi, MD, 2002, pp. 1–2.
49. Mkhize C, Britton J, Mack J and Nyokong T. *J. Porphyrins Phthalocyanines* 2015; **19**: 192–204.
50. Mkhize C, Britton J and Nyokong T. *Polyhedron* 2014; **81**: 607–613.
51. Sekhosana KE, Amuhaya E and Nyokong T. *Polyhedron* 2015; **85**: 347–354.